IRS-Assisted Downlink and Uplink NOMA in Wireless Powered Communication Networks

Journal:	*IEEE Transactions on Vehicular Technology*
Manuscript ID	VT-2021-01665
Suggested Category:	Correspondence
Date Submitted by the Author:	17-May-2021
Complete List of Authors:	Lyu, Bin; Nanjing University of Posts and Telecommunications Ramezani, Parisa; Univ. of Sydney, Electrical & Information Engineering Dinh , Hoang; University of Technology Sydney, School of Electrical and Data Engineering Jamalipour, Abbas; Univ. of Sydney, Electrical & Information Engineering
Keywords:	Wireless powered communication network, Non-orthogonal multiple access, Intelligent reflecting surface

IRS-Assisted Downlink and Uplink NOMA in Wireless Powered Communication Networks

Bin Lyu, Parisa Ramezani, Dinh Thai Hoang, and Abbas Jamalipour

***Abstract*—This paper studies the integration of the newly-emerged intelligent reflecting surface (IRS) technology into non-orthogonal multiple access (NOMA)-based wireless powered communication networks (WPCNs). We consider two WPCNs which communicate with a common hybrid access point (HAP), where there exists two types of devices in each WPCN, namely information receiving device (IRD) and harvest-then-transmit device (HTTD). Downlink communication from the HAP to IRDs, downlink energy transfer (ET) from the HAP to HTTDs, and uplink information transmission from the HTTDs to the HAP are assisted by two IRSs, one in each WPCN. Under this setup, we propose efficient algorithms to optimize reflection coefficients, beamforming vectors, and resource allocation for the sake of uplink sum-rate maximization, taking into account the minimum rate requirement at the IRDs. Numerical results show the considerable performance gain of the proposed NOMA-based scheme as compared to the conventional orthogonal multiple access (OMA)-based counterpart.**

***Index Terms*—Wireless powered communication network, non-orthogonal multiple access, intelligent reflecting surface.**

I. Introduction

Intelligent reflecting surface (IRS) has recently come on the scene as a means to control the behavior of wireless channels, which can electronically modify the phase and amplitude of the incident signals and reflect them in the desired direction [1]. This ground-breaking technology has lately been studied by many researchers and proved to offer significant performance gains for the existing wireless communication networks [2], [3]. Although foreseen as a key enabler of 6G wireless systems, IRS cannot be a game-changer on its own. This paradigm needs to be studied in combination with other technologies to be able to fulfill the promises of 6G [2].

Wireless powered communication network (WPCN) has gained much interest in the past decade as the key technology for facilitating the realization of the Internet of Things (IoT) [4]. However, WPCN suffers from low spectral efficiency because the harvest-then-transmit devices (HTTDs) prefer to use the time division multiple access (TDMA) protocol to avoid interference. To address this issue, the integration of WPCN and NOMA has been studied, which demonstrated promising results for performance gain [5]. However, the performance enhancement may still be limited due to the low downlink energy transfer (ET) efficiency from the hybrid access point (HAP) to the HTTDs, which results in low uplink information transmission (IT) rates. Inspired by its unique properties, IRS has been recently employed in NOMA-based WPCNs to further boost the performance of downlink ET and uplink IT [6], [7]. However, these works assumed a single-antenna HAP and ignored the performance enhancements that can be achieved by the optimal design of active beamforming at the HAP. More importantly, unlike what has been considered in [5]–[7] and many other works on WPCNs, the operation of the HAP should not be limited by downlink ET and uplink information reception only. Instead, the downlink IT to information receiving devices (IRDs) should be also taken into consideration.

In this paper, we propose a novel framework for IRS-empowered NOMA-based WPCNs, where two hybrid WPCNs, each having one IRD, one HTTD and an IRS, communicate with a common HAP. Specifically, the HAP first performs simultaneous IT and ET in the downlink by transmitting information signals via NOMA to the IRDs, where the signals are also used by the HTTDs for energy harvesting (EH). Each IRS is employed to assist both downlink IT from the HAP to the IRD and downlink ET from the HAP to the HTTD in its WPCN. Then, the HTTDs transmit their information to the HAP using NOMA with the assistance of IRSs. We investigate the uplink sum-rate maximization problem under the minimum rate constraint at IRDs, energy causality constraint at HTTDs, and maximum transmit power constraint at the HAP. It should be noted that unlike [6], [7], our formulated problem is more challenging to solve due to the minimum rate constraint at the IRDs and joint optimization of active and passive beamforming. We thus propose an alternating algorithm to solve the formulated problem efficiently. In particular, we obtain the closed-form expression for uplink amplitude reflection coefficients and phase shifts, use the semidefinite relaxation (SDR) technique to optimize the downlink reflection coefficients and active beamforming vectors, and further discuss the properties of active beamforming. Numerical results show that our proposed scheme significantly enhances the uplink sum-rate, while efficiently meeting the downlink rate requirements.

II. System Model

As illustrated in Fig. 1, we consider a joint downlink and uplink IRS-assisted NOMA network, consisting of one near-WPCN and one far-WPCN. Each WPCN comprises one IRD, one HTDD, and one IRS with N reflecting elements. The HAP has M antennas and devices have one single antenna each.

B. Lyu is with Nanjing University of Posts and Telecommunications, Nanjing 210003, China (email: blyu@njupt.edu.cn).

P. Ramezani and A. Jamalipour are with University of Sydney, Sydney, NSW 2006, Australia (email: parisa.ramezani@sydney.edu.au, a.jamalipour@ieee.org)

D. T. Hoang is with University of Technology Sydney, Sydney, NSW 2007, Australia (email: hoang.dinh@uts.edu.au).

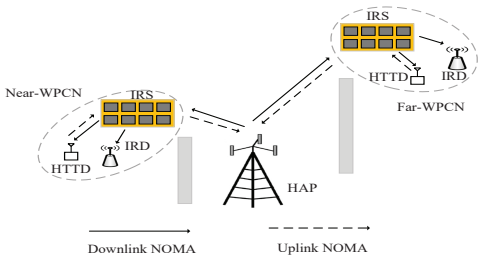

Fig. 1. Joint downlink and uplink IRS-assisted NOMA network.

The HAP is embedded with sufficient energy supply, while each HTTD is equipped with an EH circuit to harvest energy from ET of the HAP.[1] The direct links between devices and the HAP are unavailable due to the blockages [8]. Thus, both downlink and uplink communications in each WPCN can only be performed through the corresponding IRS.

We consider a unit transmission block (or a time frame), which is divided into two phases, i.e., downlink NOMA phase and uplink NOMA phase. In the first phase, the HAP transmits information signals to the IRDs in the downlink using NOMA. The downlink transmitted signals of the HAP are also used by the HTTDs for EH. In the second phase, the HTTDs simultaneously transmit their own information signals to the HAP in the uplink.

A. Downlink NOMA Phase

In the downlink NOMA phase with duration of $1-\beta$, the HAP transmits superposition signals to the IRDs with the assistance of their corresponding IRSs. Denote the superposition signal as $\boldsymbol{w}_{\text{near},d}s_{\text{near},d}+\boldsymbol{w}_{\text{far},d}s_{\text{far},d}$, where $\boldsymbol{w}_{j,d}$ is the transmit beamforming vector for the IRD in j-WPCN ($j\in\{\text{near},\text{far}\}$) and $s_{j,d}$ is the unit-power signal to be sent to the j-IRD. The downlink reflection matrix of the j-IRS is denoted by $\boldsymbol{\Theta}_{j,d}=\text{diag}\{\alpha_{j,d,1}e^{i\theta_{j,d,1}},\ldots,\alpha_{j,d,N}e^{i\theta_{j,d,N}}\}$ (with i denoting the imaginary unit), where $\alpha_{j,d,n}\in[0,1]$ and $\theta_{j,d,n}\in[0,2\pi)$ are the amplitude reflection coefficient and phase shift of the n-th element in the downlink communication, respectively. The received signal at the j-IRD is given by

$$y_{j,r}=\boldsymbol{h}_{j,r}^H\boldsymbol{\Theta}_{j,d}\boldsymbol{H}_j(\boldsymbol{w}_{\text{near},d}s_{\text{near},d}+\boldsymbol{w}_{\text{far},d}s_{\text{far},d})+n_{j,r}, \quad (1)$$

where $\boldsymbol{h}_{j,r}^H\in C^{1\times N}$ is the channel from the IRS to the IRD in the j-WPCN, $\boldsymbol{H}_j\in C^{N\times M}$ is the channel from the HAP to the j-IRS, and $n_{j,d}\sim\mathcal{CN}(0,\sigma_{j,d}^2)$ is the additive white Gaussian noise (AWGN) at the j-IRD.

Without loss of generality, we assume the channel condition between the HAP and near-IRD is better than that of the HAP and far-IRD, and the successive interference cancellation (SIC) is only applied in the near-WPCN to eliminate the interference from the far-WPCN [8], [9]. This is a reasonable assumption considering the effect of distance on channel conditions. Hence, the IRD in the far-WPCN decodes its signal directly and the corresponding SINR is expressed as $\text{SINR}_{\text{far}}=\frac{|\boldsymbol{h}_{\text{far},r}^H\boldsymbol{\Theta}_{\text{far},d}\boldsymbol{H}_{\text{far}}\boldsymbol{w}_{\text{far},d}|^2}{|\boldsymbol{h}_{\text{far},r}^H\boldsymbol{\Theta}_{\text{far},d}\boldsymbol{H}_{\text{far}}\boldsymbol{w}_{\text{near},d}|^2+\sigma_{\text{far},r}^2}$.

[1]The IRDs are typically information receivers. However, they can also be equipped with the EH circuit to harvest energy from receiving signals to sustain their operations.

The IRD in the near-WPCN applies SIC to decode the signal of the IRD in the far-WPCN first and then removes the interference. The SINR to decode the signal of the far-IRD in the near-WPCN is given by $\text{SINR}_{\text{near}\to\text{far}}=\frac{|\boldsymbol{h}_{\text{near},r}^H\boldsymbol{\Theta}_{\text{near},d}\boldsymbol{H}_{\text{near}}\boldsymbol{w}_{\text{far},d}|^2}{|\boldsymbol{h}_{\text{near},r}^H\boldsymbol{\Theta}_{\text{near},d}\boldsymbol{H}_{\text{near}}\boldsymbol{w}_{\text{near},d}|^2+\sigma_{\text{near},r}^2}$. After that, the SNR of the IRD in the near-WPCN to decode its own signal is expressed as $\text{SNR}_{\text{near}}=\frac{|\boldsymbol{h}_{\text{near},r}^H\boldsymbol{\Theta}_{\text{near},d}\boldsymbol{H}_{\text{near}}\boldsymbol{w}_{\text{near},d}|^2}{\sigma_{\text{near},r}^2}$.

The achievable rates of the two IRDs can be expressed as

$$R_{\text{near,d}}=(1-\beta)\log_2(1+\text{SINR}_{\text{near}}), \quad (2)$$

$$R_{\text{far,d}}=(1-\beta)\log_2(1+\min\{\text{SINR}_{\text{near}\to\text{far}},\text{SINR}_{\text{far}}\}). \quad (3)$$

The received signal at the HTTD in j-WPCN is given by

$$y_{j,h}=\boldsymbol{h}_{j,h}^H\boldsymbol{\Theta}_{j,d}\boldsymbol{H}_j(\boldsymbol{w}_{\text{near},d}s_{\text{near},d}+\boldsymbol{w}_{\text{far},d}s_{\text{far},d})+n_{j,h}, \quad (4)$$

where $\boldsymbol{h}_{j,h}^H\in C^{1\times N}$ is the channel from the IRS to the HTTD in the j-WPCN and $n_{j,h}\sim\mathcal{CN}(0,\sigma_{j,h}^2)$ is the AWGN at the j-HTTD. The received power at the HTTD in the j-WPCN is thus given by $P_{j,h}=|\boldsymbol{h}_{j,h}^H\boldsymbol{\Theta}_{j,d}\boldsymbol{H}_j\boldsymbol{w}_{\text{near},d}|^2+|\boldsymbol{h}_{j,h}^H\boldsymbol{\Theta}_{j,d}\boldsymbol{H}_j\boldsymbol{w}_{\text{far},d}|^2$. Note that the noise power is very small for EH and can be neglected. To capture the EH characteristics at the HTTDs, the practical two-piece linear EH model [10] is considered, following which the harvested energy by the HTTD in the j-WPCN is calculated as $E_{j,h}=\min\{\eta P_{j,h},P_{\text{sat}}\}(1-\beta)$, where η is the EH efficiency in the linear regime and P_{sat} denotes the saturation power, i.e., maximum harvestable power.

B. Uplink NOMA Phase

In the uplink NOMA phase with duration of β, the HTTDs use their harvested energy to transmit signals to the HAP simultaneously. Denote the transmit signal of HTTD in the j-WPCN as $\sqrt{P_{j,u}}s_{j,u}$, where $s_{j,u}$ is the information-carrying signal with unit power, $P_{j,u}$ is the transmit power and satisfies $(P_{j,u}+P_{c,u})\beta\le E_{j,h}$, with $P_{c,u}$ being the circuit power consumption of the HTTDs.

Denote the uplink reflection matrix of the j-IRS as $\boldsymbol{\Theta}_{j,d}=\text{diag}\{\alpha_{j,u,1}e^{i\theta_{j,u,1}},\ldots,\alpha_{j,u,N}e^{i\theta_{j,u,N}}\}$, where $\alpha_{j,u,n}\in[0,1]$ and $\theta_{j,u,n}\in[0,2\pi)$ respectively represent the amplitude reflection coefficient and phase shift of the n-th element in the uplink communication. The received signal at the HAP is expressed as $y_h=\boldsymbol{G}_{\text{near}}^H\boldsymbol{\Theta}_{\text{near},u}\boldsymbol{g}_{\text{near},h}\sqrt{P_{\text{near},u}}s_{\text{near},u}+\boldsymbol{G}_{\text{far}}^H\boldsymbol{\Theta}_{\text{far},u}\boldsymbol{g}_{\text{far},h}\sqrt{P_{\text{far},u}}s_{\text{far},u}+n_h$, where $\boldsymbol{G}_j^H\in C^{M\times N}$ denotes the channel from the j-IRS to the HAP, $\boldsymbol{g}_{j,h}\in C^{N\times 1}$ denotes the channel from the HTTD to the IRS in the j-WPCN, and $n_h\sim\mathcal{CN}(0,\sigma_h^2)$ is the AWGN at the HAP. Similarly, we assume that the channel condition between the HAP and near-HTTD is better than that of the HAP and far-HTTD [6]. By using the minimum mean square error (MMSE) detector, the HAP first detects and decodes the signal from the near-HTTD. Then, the HAP cancels the decoded signal from the received signal and detects the far-HTTD's signal. The uplink sum-rate in the second phase is thus given by

$$R=\beta\log_2\det\left(\boldsymbol{I}_M+(P_{\text{near},u}\bar{\boldsymbol{g}}_{\text{near}}\bar{\boldsymbol{g}}_{\text{near}}^H+P_{\text{far},u}\bar{\boldsymbol{g}}_{\text{far}}\bar{\boldsymbol{g}}_{\text{far}}^H)/\sigma_h^2\right) \quad (5)$$

where $\bar{\boldsymbol{g}}_j=\boldsymbol{G}_j^H\boldsymbol{\Theta}_{j,u}\boldsymbol{g}_{j,h}\in C^{M\times 1}$.

III. Uplink Sum-Rate Maximization

In this section, we aim to maximize the uplink sum-rate under the QoS constraints at the IRDs. In particular, the achievable rates at the IRDs should satisfy the constraints: C1: $R_{\text{near},d} \geq R_{\text{near, min}}$ and C2: $R_{\text{far},d} \geq R_{\text{far,min}}$, where $R_{\text{near,min}}$ and $R_{\text{far,min}}$ are the minimum data rates required at the IRDs. We also have the energy causality constraint at the HTTDs as C3: $(P_{j,u} + P_{j,c})\beta \leq E_{j,h}$ and the maximum transmit power constraint at the HAP as C4: $||\boldsymbol{w}_{\text{near},d}||^2 + ||\boldsymbol{w}_{\text{far},d}||^2 \leq P_{\max}$. Other constraints about time and power allocation and relfection coefficients are as follows: C5: $0 \leq \beta \leq 1$, C6: $0 \leq \alpha_{j,d,n} \leq 1$, $\forall n$, C7: $0 \leq \theta_{j,d,n} < 2\pi$, $\forall n$, C8: $0 \leq \alpha_{j,u,n} \leq 1$, $\forall n$, C9: $0 \leq \theta_{j,u,n} < 2\pi$, $\forall n$, and C10: $P_{j,u} \geq 0$. Under these constraints, the optimization problem is formulated as

$$\max_{\substack{\boldsymbol{w}_{j,d}, P_{j,u}, \beta, \\ \alpha_{j,u,n}, \alpha_{j,d,n}, \theta_{j,u,n}, \theta_{j,d,n}}} \quad R, \quad \text{s.t. C1} - \text{C10}. \tag{P1}$$

It is straightforward that **P1** is a non-convex optimization problem due to the coupled variables in the objective function and constraints, and thus it is very difficult to obtain the globally optimal solution by conventional convex optimizers. In the following, we propose an efficient algorithm based on block coordinate descent (BCD) to find the near-optimal solution to **P1**.

Prior to solving **P1**, we first check its feasibility, i.e., whether the QoS constraints at the IRDs (i.e., C1 and C2) can be met. It is straightforward to observe that **P1** is feasible if and only if its feasibility is guaranteed by ignoring the HTTDs, i.e., letting $\beta = 0$. In this regard, we introduce an auxiliary variable δ, and formulate the feasibility check problem as

$$\begin{aligned} &\min_{\boldsymbol{w}_{j,d}, \alpha_{j,d,n}, \theta_{j,d,n}} \quad \delta, \\ &\text{s.t. C4, C6, C7,} \\ &\quad R_{\text{near},d} + \delta \geq R_{\text{near,min}}, \ R_{\text{far},d} + \delta \geq R_{\text{far,min}}. \end{aligned} \tag{P2}$$

Similar to **P1**, **P2** is non-convex and can be solved by the BCD based algorithm, the details of which will be elaborated in the following subsections (see Algorithm 1 for details). If the obtained δ is not greater than zero, the original problem, i.e., **P1**, is feasible. In the following, we will explain the steps for solving the uplink sum-rate maximization in our proposed IRS-assisted NOMA-based network.

A. Uplink Reflection Optimization

Here, we aim to optimize the reflection coefficients of IRSs in uplink IT, with other variables being fixed. To this end, we propose a two-layer alternating optimization framework. In the outer-layer loop, we iteratively optimize the reflection coefficients of one IRS with the reflection coefficients of the other IRS being fixed, while we have two inner-layer loops, each for alternative optimization of the individual reflection coefficients of the corresponding IRS. Setting $\boldsymbol{v}_{j,u} = [\alpha_{j,u,1}e^{i\theta_{j,u,1}}, ..., \alpha_{j,u,N}e^{i\theta_{j,u,N}}]^T$, $\boldsymbol{\psi}_j = \boldsymbol{G}_j^H \text{diag}(\boldsymbol{g}_{j,h})$, and using the product rule of logarithms and Sylvester's determinant identity, the expression in (5) can be rewritten as $R = \log_2(1 + \boldsymbol{v}_{\text{far},u}^H \boldsymbol{A}_{\text{far}} \boldsymbol{v}_{\text{far},u}) + \log_2 \det(\boldsymbol{I}_M + \frac{P_{\text{near}}}{\sigma_h^2} \boldsymbol{\psi}_{\text{near}} \boldsymbol{v}_{\text{near}} \boldsymbol{v}_{\text{near}}^H \boldsymbol{\psi}_{\text{near}}^H)$, where $\boldsymbol{A}_{\text{far}} = \boldsymbol{C}_{\text{far}}^H \boldsymbol{C}_{\text{far}}$, $\boldsymbol{C}_{\text{far}} = \sqrt{P_{\text{far}}/\sigma_h^2}(\boldsymbol{I}_M + \frac{P_{\text{near}}}{\sigma_h^2} \boldsymbol{\psi}_{\text{near}} \boldsymbol{v}_{\text{near},u} \boldsymbol{v}_{\text{near},u}^H \boldsymbol{\psi}_{\text{near}}^H)^{-\frac{1}{2}} \boldsymbol{\psi}_{\text{far}}$.

Fixing $\boldsymbol{v}_{\text{near,u}}$, the problem for finding the far-IRS reflection coefficients is formulated as

$$\max_{\alpha_{\text{far},u,n}, \theta_{\text{far},u,n}} \ \text{Tr}(\boldsymbol{v}_{\text{far},u}^H \boldsymbol{A}_{\text{far}} \boldsymbol{v}_{\text{far},u}), \ \text{s.t.} \quad \text{C8, C9.} \tag{P3}$$

We solve **P3** by iteratively optimizing the reflection coefficient of each IRS element, given fixed values of other reflection coefficients. Specifically, the problem for optimizing the reflection coefficient of the n-th element of the far-IRS is formulated as

$$\begin{aligned} &\max_{\alpha_{\text{far},u,n}, \theta_{\text{far},u,n}} \quad A_{\text{far},n,n}\alpha_{\text{far},u,n}^2 + 2\text{Re}(b_{\text{far},n}^H \alpha_{\text{far},u,n} e^{i\theta_{\text{far},u,n}}), \\ &\text{s.t. C8, C9,} \end{aligned} \tag{P4}$$

where $A_{\text{far},n,n}$ is the n-th diagonal element of $\boldsymbol{A}_{\text{far}}$, and $b_{\text{far},n} = \sum_{m=1,m\neq n}^{N} \alpha_{\text{far},u,m} e^{i\theta_{\text{far},u,m}} A_{\text{far},m,n}$.

Proposition 1. *Given $\{\alpha_{far,u,m}, \theta_{far,u,m}\}$, $\forall m \neq n$, the optimal amplitude reflection coefficient and phase shift of **P4** are given by $\alpha_{far,u,n}^* = 1$ and $\theta_{far,u,n}^* = arg(b_{far,n})$, where $arg(x)$ denotes the phase of x.*

By sequentially optimizing $\alpha_{\text{far},u,n}$ and $\theta_{\text{far},u,n}$ for $n = 1, \ldots, N$ in an iterative manner, we can finally find the near-optimal solution to **P3**. We can then follow a similar procedure for optimizing the reflection coefficients of the near-IRS, with $\boldsymbol{v}_{\text{far},u}$ being fixed.

From Proposition 1, we can observe that to achieve the uplink maximum sum-rate, the IRSs should reflect all incident signals to enhance the received power at the HAP. For $M = 1$, the optimal uplink phase shift of the n-element of the j-IRS is given by $\theta_{j,u,n}^* = -\arg(\boldsymbol{G}_{j,n}^H) - \arg(\boldsymbol{g}_{j,h,n})$, $\forall n$, where $\boldsymbol{G}_{j,n}^H$ is the n-th element of $\boldsymbol{G}_j^H$, $\boldsymbol{g}_{j,h,n}$ is the n-th element of $\boldsymbol{g}_{j,h}$

B. Downlink Phase Shifts and Power Optimization

Now, we optimize the downlink reflection coefficients and power allocation at the HTTDs for the given β, $\boldsymbol{w}_{j,d}$, and $\boldsymbol{v}_{j,u}$. Setting $\boldsymbol{v}_{j,d} = [\alpha_{j,d,1}e^{i\theta_{j,d,1}}, ..., \alpha_{j,d,N}e^{i\theta_{j,d,N}}]^H$, and introducing $\boldsymbol{V}_{j,d} = \boldsymbol{v}_{j,d}\boldsymbol{v}_{j,d}^H$ with $\boldsymbol{V}_{j,d} \succeq 0$ and $\text{rank}(\boldsymbol{V}_{j,d}) = 1$. Let $\boldsymbol{\phi}_{\text{near},n,i} = \text{diag}(\boldsymbol{h}_{\text{near},i}^H)\boldsymbol{H}_{\text{near}}\boldsymbol{w}_{\text{near},d}$, $\boldsymbol{\phi}_{\text{near},f,i} = \text{diag}(\boldsymbol{h}_{\text{near},i}^H)\boldsymbol{H}_{\text{near}}\boldsymbol{w}_{\text{far},d}$, $\boldsymbol{\phi}_{\text{far},n,i} = \text{diag}(\boldsymbol{h}_{\text{far},i}^H)\boldsymbol{H}_{\text{far}}\boldsymbol{w}_{\text{near},d}$, and $\boldsymbol{\phi}_{\text{far},f,i} = \text{diag}(\boldsymbol{h}_{\text{far},i}^H)\boldsymbol{H}_{\text{far}}\boldsymbol{w}_{\text{far},d}$, where $i \in \{h, r\}$. Based on the new variables, the constraints C1-C3 can be recast as

$$\begin{aligned}
&\text{C9: } \text{Tr}(\boldsymbol{V}_{\text{near},d}\boldsymbol{\phi}_{\text{near},n,r}\boldsymbol{\phi}_{\text{near},n,r}^H) \geq (2^{(R_{\text{near,min}}/(1-\beta))} - 1)\sigma_{\text{near},r}^2, \\
&\text{C10: } \text{Tr}(\boldsymbol{V}_{\text{far},d}\boldsymbol{\phi}_{\text{far},f,r}\boldsymbol{\phi}_{\text{far},f,r}^H) \geq (2^{(R_{\text{far,min}}/(1-\beta))} - 1) \\
&\qquad \times [\text{Tr}(\boldsymbol{V}_{\text{far},d}\boldsymbol{\phi}_{\text{far},n,r}\boldsymbol{\phi}_{\text{far},n,r}^H) + \sigma_{\text{far},r}^2], \\
&\text{C11: } \text{Tr}(\boldsymbol{V}_{\text{near},d}\boldsymbol{\phi}_{\text{near},f,r}\boldsymbol{\phi}_{\text{near},f,r}^H) \geq (2^{R_{\text{far,min}}/(1-\beta)} - 1) \\
&\qquad \times [\text{Tr}(\boldsymbol{V}_{\text{near},d}\boldsymbol{\phi}_{\text{near},n,r}\boldsymbol{\phi}_{\text{near},n,r}^H) + \sigma_{\text{near},r}^2], \\
&\text{C12: } (P_{\text{near},u} + P_{\text{near},c})\beta \leq \min\{\eta\text{Tr}(\boldsymbol{V}_{\text{near},d}\boldsymbol{\phi}_{\text{near},n,h}\boldsymbol{\phi}_{\text{near},n,h}^H) \\
&\qquad + \eta\text{Tr}(\boldsymbol{V}_{\text{near},d}\boldsymbol{\phi}_{\text{near},f,h}\boldsymbol{\phi}_{\text{near},f,h}^H), P_{\text{sat}}\}(1-\beta), \\
&\text{C13: } (P_{\text{far},u} + P_{\text{far},c})\beta \leq \min\{\eta\text{Tr}(\boldsymbol{V}_{\text{far},d}\boldsymbol{\phi}_{\text{far},n,h}\boldsymbol{\phi}_{\text{far},n,h}^H) \\
&\qquad + \eta\text{Tr}(\boldsymbol{V}_{\text{far},d}\boldsymbol{\phi}_{\text{far},f,h}\boldsymbol{\phi}_{\text{far},f,h}^H), P_{\text{sat}}\}(1-\beta).
\end{aligned}$$

The optimal downlink reflection coefficients and power allocation can be found by solving the following problem

$$\begin{aligned} \max_{\boldsymbol{V}_{j,d}, P_{j,u}} \quad & R, \\ \text{s.t.} \quad & \text{C9} - \text{C13}, \ \boldsymbol{V}_{j,d,n,n} \le 1, \ \forall n, \\ & \boldsymbol{V}_{j,d} \succeq 0, \ \text{rank}(\boldsymbol{V}_{j,d}) = 1. \end{aligned} \tag{P5}$$

P5 is still non-convex due to the rank-one constraints. By employing the SDR technique to relax the rank-one constraint, **P5** can be transformed into a convex semidefinite programming (SDP) problem [11], which can be optimally solved by convex solvers, e.g., CVX [12]. However, the solution obtained by CVX may not satisfy the rank-one constraint, in which case we can employ the Gaussian randomization technique to construct a rank-one solution and finally extract $\boldsymbol{v}_{j,d}$.

C. Transmit Beamforming Optimization

We then optimize the transmit beamforming vectors for the given β, $\boldsymbol{v}_{j,d}$, $\boldsymbol{v}_{j,u}$, and $P_{j,u}$. Letting $\boldsymbol{W}_{j,d} = \boldsymbol{w}_{j,d}\boldsymbol{w}_{j,d}^H$, where $\boldsymbol{W}_{j,d} \succeq 0$ and $\text{rank}(\boldsymbol{W}_{j,d}) = 1$, $\bar{\boldsymbol{h}}_{j,h}^H = \boldsymbol{h}_{j,h}^H \boldsymbol{\Theta}_{j,d} \boldsymbol{H}_j$, and $\bar{\boldsymbol{h}}_{j,r}^H = \boldsymbol{h}_{j,r}^H \boldsymbol{\Theta}_{j,d} \boldsymbol{H}_j$, the constraints C1-C4 can be rewritten as

$$\text{C14: } \text{Tr}(\bar{\boldsymbol{h}}_{\text{near},r} \bar{\boldsymbol{h}}_{\text{near},r}^H \boldsymbol{W}_{\text{near},d}) \ge (2^{R_{\text{near,min}}/(1-\beta)} - 1)\sigma_{\text{near},r}^2,$$

$$\begin{aligned} \text{C15: } & \text{Tr}(\bar{\boldsymbol{h}}_{\text{far},r} \bar{\boldsymbol{h}}_{\text{far},r}^H \boldsymbol{W}_{\text{far},d}) \ge \\ & (2^{R_{\text{far,min}}/(1-\beta)} - 1)[\text{Tr}(\bar{\boldsymbol{h}}_{\text{far},r} \bar{\boldsymbol{h}}_{\text{far},r}^H \boldsymbol{W}_{\text{near},d}) + \sigma_{\text{far},r}^2], \end{aligned}$$

$$\begin{aligned} \text{C16: } & \text{Tr}(\bar{\boldsymbol{h}}_{\text{near},r} \bar{\boldsymbol{h}}_{\text{near},r}^H \boldsymbol{W}_{\text{far},d}) \ge \\ & (2^{R_{\text{far,min}}/(1-\beta)} - 1)[\text{Tr}(\bar{\boldsymbol{h}}_{\text{near},r} \bar{\boldsymbol{h}}_{\text{near},r}^H \boldsymbol{W}_{\text{near},d}) + \sigma_{\text{near},r}^2], \end{aligned}$$

$$\begin{aligned} \text{C17: } & (P_{j,u} + P_{j,c})\beta \le \\ & \min\left\{\eta[\text{Tr}(\bar{\boldsymbol{h}}_{j,h} \bar{\boldsymbol{h}}_{j,h}^H \boldsymbol{W}_{\text{near},d}) + \text{Tr}(\bar{\boldsymbol{h}}_{j,h} \bar{\boldsymbol{h}}_{j,h}^H \boldsymbol{W}_{\text{far},d})], P_{\text{sat}}\right\}(1-\beta), \end{aligned}$$

$$\text{C18: } \text{Tr}(\boldsymbol{W}_{\text{near},d}) + \text{Tr}(\boldsymbol{W}_{\text{far},d}) \le P_{\max}.$$

With the new constraints, P1 can be transformed into a feasibility problem, which is given by

$$\begin{aligned} \text{find} \quad & \boldsymbol{W}_{j,d}, \\ \text{s.t.} \quad & \text{C14} - \text{C18}, \\ & \boldsymbol{W}_{j,d} \succeq 0, \ \text{rank}(\boldsymbol{W}_{j,d}) = 1, j \in \{\text{near}, \text{far}\}. \end{aligned} \tag{P6}$$

Again, we can apply the SDR technique to remove the rank-one constraint and use CVX to solve the relaxed problem optimally. Denote the optimal solution to the relaxed problem as $\boldsymbol{W}_{\text{near},d}^*$ and $\boldsymbol{W}_{\text{far},d}^*$. According to Theorem 3.2 in [13], $\boldsymbol{W}_{\text{near},d}^*$ and $\boldsymbol{W}_{\text{far},d}^*$ should satisfy the following constraint:

$$[\text{rank}(\boldsymbol{W}_{\text{near},d}^*)]^2 + [\text{rank}(\boldsymbol{W}_{\text{far},d}^*)]^2 \le 6. \tag{6}$$

It is obvious that $\boldsymbol{W}_{\text{near},d}^* \ne \boldsymbol{0}$ and $\boldsymbol{W}_{\text{far},d}^* \ne \boldsymbol{0}$. Hence, we can obtain that at least one of the transmit beamforming matrices is rank-one, i.e., $\text{rank}(\boldsymbol{W}_{j,d}^*) = 1$ and $\text{rank}(\boldsymbol{W}_{\lambda \ne j,d}^*) = 1$or 2 [8]. If $\text{rank}(\boldsymbol{W}_{j,d}^*) = 1$, we can use the SVD to achieve the optimal transmit beamforming vector $\boldsymbol{v}_{j,d}^*$. Otherwise, we can use Gaussian randomization method to construct a rank-one solution with satisfying accuracy.

Under the condition that $\eta P_{j,h} \ge P_{\text{sat}}$, the constraint C17 can be simplified as $(P_{j,u} + P_{j,c})\beta \le P_{\text{sat}}(1-\beta)$. For this case, the constraint in (6) can be rewritten as

$$[\text{rank}(\boldsymbol{W}_{\text{near},d}^*)]^2 + [\text{rank}(\boldsymbol{W}_{\text{far},d}^*)]^2 \le 4, \tag{7}$$

in which case both $\boldsymbol{W}_{\text{near},d}^*$ and $\boldsymbol{W}_{\text{far},d}^*$ are rank-one.

In addition, for the case without considering the QoS constraints at the IRDs, we can obtain that $\boldsymbol{W}_{\text{near},d} = \boldsymbol{W}_{\text{far},d}$ and $\text{rank}(\boldsymbol{W}_{j,d}) = 1$ [13].

Finally, we can find β by the one-dimensional search. In summary, the steps for solving **P1** are given in Algorithm 1. As the objective function of **P1** increases after each update and is bounded from above, the convergence of the algorithm is guaranteed.

Algorithm 1 The Algorithm for Solving **P1**.

Let $\beta = 0$. Initialize the step size Δ.
while $\beta < 1$ **do**
  Check the feasibility of **P1** by solving **P2**.
  if P1 is feasible **then**
    Initialize $\boldsymbol{w}_{j,d}$, $\boldsymbol{v}_{j,d}$, and $P_{j,u}$.
    Initialize $\boldsymbol{v}_{\text{near},u}$ and $\boldsymbol{v}_{\text{far},u}$.
    repeat
      repeat
        Compute $\boldsymbol{A}_{\text{far}}$.
        repeat
          Update $\alpha_{\text{far},u,n}$ and $\theta_{\text{far},u,n}$ according to Proposition 1.
        until the convergence is achieved.
        Compute $\boldsymbol{A}_{\text{near}}$.
        repeat
          Update $\alpha_{\text{near},u,n}$ and $\theta_{\text{near},u,n}$.
        until the convergence is achieved.
      until the convergence is achieved.
      Update $\boldsymbol{v}_{j,d}$ and $P_{j,u}$ by solving **P5** with fixed β, $\boldsymbol{v}_{j,u}$, and $\boldsymbol{w}_{j,d}$.
      Update $\boldsymbol{w}_{j,d}$ by solving **P6** with fixed β, $\boldsymbol{v}_{j,u}$, $\boldsymbol{v}_{j,d}$, and $P_{j,u}$.
    until the convergence is achieved.
    Obtain $R(\beta)$.
  else
    Break the loop.
  end if
  $\beta = \beta + \Delta$.
end while
Set $\beta^* = \arg\max_\beta R$, $\boldsymbol{v}_{j,u}^* = \boldsymbol{v}_{j,u}(\beta^*)$, $\boldsymbol{v}_{j,d}^* = \boldsymbol{v}_{j,d}(\beta^*)$, $\boldsymbol{w}_{j,d}^* = \boldsymbol{w}_{j,d}(\beta^*)$, and $P_{j,u}^* = P_{j,u}(\beta^*)$.

IV. Numerical Results

In this section, we further evaluate the system performance by numerical results. The distances between the HAP and the near-IRS and far-IRS, denoted by d_{near} and d_{far}, are set at $d_{\text{near}} = 2$ m and $d_{\text{far}} = 6$ m, respectively. In each WPCN, the HTTD and IRD are randomly and uniformly distributed within a radius of 1 m centered at their IRSs. The large-scale fading follows the model $\mathcal{A}(d)^{-\rho}$, where $\mathcal{A}$ is the path-loss at the reference distance of 1 meter and set as $\mathcal{A} = -20$ dB, ρ is the path-loss exponent and set as 2.2, d is the distance between two nodes. In addition, Rayleigh fading is used to model the small-scale fading for all channels [7]. Other parameters are given as follows: $R_{\text{near,min}} = 5$ bits/Hz, $R_{\text{far,min}} = 2$ bits/Hz, $P_{\text{sat}} = 10$ mW, $P_{\max} = 20$ dBm, $P_{j,c} = 5$ mW, $M = 4$, $N = 20$, $\eta = 0.8$, $\sigma_h^2 = \sigma_{j,r} = -70$ dBm. We compare the performance of our proposed scheme with 1) the scheme with random reflection coefficients for IRSs, 2) OMA-based

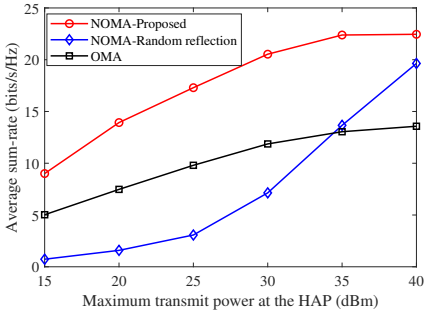

Fig. 2. Sum-rate versus the HAP's maximum transmit power.

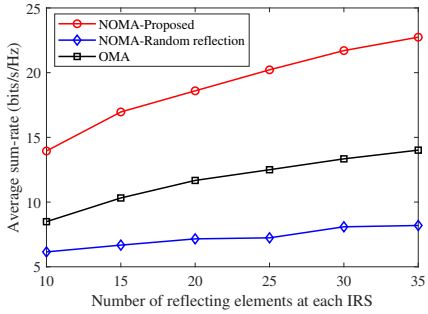

Fig. 3. Sum-rate versus the number of each IRS's reflecting elements.

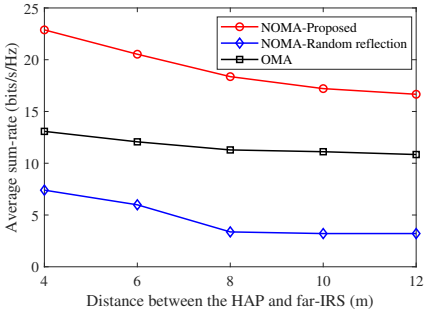

Fig. 4. Sum-rate versus the distance of the far-IRS.

scheme, where TDMA is used for both uplink and downlink IT.

In Fig. 2, we investigate the effect of the maximum transmit power at the HAP on the average sum-rate. It is straightforward that the average sum-rate increases with the increase of the HAP's maximum transmit power. The reason is that more power can be harvested by the HTTDs and more time can be allocated to the HTTDs for IT since the downlink NOMA phase can be completed in shorter time. In addition, we can find that the proposed scheme remarkably outperforms the benchmarks. When $P_{\max} \geq 35$ dBm, the average sum-rate achieved by the proposed scheme tends to be saturated as the harvested power at the HTTDs reaches the saturation limit. When $P_{\max}$ is small, the sum-rate achieved by the scheme with random reflection is very low because with non-optimized IRS reflection coefficients, most of the time is spent for meeting the QoS constraints at the IRDs, leaving very limited time for the uplink IT of the HTTDs. In addition, it may happen that the QoS constraints at the IRDs cannot be met even if all the time is allocated to the downlink phase.

Fig. 3 shows the effect of the number of reflecting elements at each IRS on the average sum-rate. With the increase of number of reflecting elements, the sum-rates of all schemes improve, because more ET and IT links are provided between the HAP and the HTTDs. Again, the figure demonstrates the superior performance of the proposed scheme compared to those of the benchmark schemes. For example, the average sum-rate gap between the proposed NOMA-based scheme and the OMA-based approach is 9.34 bits/s/Hz for $N = 30$. The reason is that the NOMA-based scheme utilizes the available resources more efficiently in both downlink and uplink communications.

In Fig. 4, the impact of the distance between the HAP and far-IRS on the average sum-rate is investigated. We can find that increasing the distance reduces the sum-rate since more time has to be expended to satisfy the QoS requirement of the far-IRD. In addition, a longer distance reduces the efficiency of downlink ET and uplink IT between the HAP and far-HTTD.

V. Conclusions

This paper has studied the integration of IRS with NOMA-based WPCNs, in which downlink communications from the HAP to IRDs and uplink communications from the HTTDs to the HAP are fulfilled based on the NOMA technique and with the help of IRS. The uplink sum-rate maximization problem has been investigated by seeking the optimal design for the IRS reflection coefficients, HAP transmit beamforming, users' power allocation, and time allocation for downlink and uplink transmissions, taking the QoS constraints at IRDs into consideration. The efficiency of the proposed IRS-assisted NOMA-based scheme has been validated via numerical simulations.

References

[1] C. Huang *et al.*, "Reconfigurable intelligent surfaces for energy efficiency in wireless communication," *IEEE Trans. Wireless Commun.*, vol. 18, no. 8, pp. 4157-4170, Jun. 2019.

[2] Q. Wu and R. Zhang, "Towards smart and reconfigurable environment: Intelligent reflecting surface aided wireless network," *IEEE Commun. Mag.*, vol. 58, no. 1. pp 106-112, Jan. 2020.

[3] J. -C. Chen, "Beamforming optimization for intelligent reflecting surface-aided MISO communication systems," *IEEE Trans. Veh. Tech.*, vol. 70, no. 1, pp. 504-513, Jan. 2021.

[4] P. Ramezani and A. Jamalipour, "Toward the evolution of wireless powered communication networks for the future Internet of Things," *IEEE Network*, vol. 31, no. 6, pp. 62-69, Nov./Dec. 2017.

[5] P. D. Diamantoulakis *et al.*, "Wireless-powered communications with non-orthogonal multiple access," *IEEE Trans. Wireless Commun.*, vol. 15, no. 12, pp. 8422-8436, Dec. 2016.

[6] D. Song, W. Shin, J. Lee, "A maximum throughput design for wireless powered communications networks with IRS-NOMA," *IEEE Wireless Commun. Lett.*, vol. 10, no. 4, pp. 849-853, April 2021.

[7] Q. Wu, X. Zhou, R. Schober, "IRS-assisted wireless powered NOMA: Do We Really Need Different Phase Shifts in DL and UL?" *IEEE Wireless Commun. Lett.*, Early access, 2021.

[8] F. Fang *et al.*, "Energy-efficient design of IRS-NOMA networks," *IEEE Trans. Veh. Tech.*, vol. 69, no. 11, pp. 14088-14092, Nov. 2020.

[9] X. Xie, F. Fang, and Z. Ding, "Joint optimization of beamforming, phase-shifting and power allocation in a multi-cluster IRS-NOMA network," *arXiv preprint arXiv:2009.06233,* 2020.

[10] S. Pejoski, Z. Hadzi-Velkov, and R. Schober, "Optimal power and time allocation for WPCNs with piece-wise linear EH model," *IEEE Wireless Commun. Lett.*, vol. 7, no. 3, pp. 364-367, June 2018.

[11] S. Boyd and L. Vandenberghe, *Convex Optimization*. Cambridge University Press, 2004.

[12] Michael Grant *et al.*, "CVX: Matlab software for disciplined convex programming," Available Online: http://cvxr.com/cvx, September 2013.

[13] Y. Huang and D. P. Palomar, "Rank-constrained separable semidefinite programming with applications to optimal beamforming," *IEEE Trans. Signal Process.*, vol. 58, no. 2, pp. 664–678, Feb. 2010.